THE JOURNAL OF BIOLOGICAL CHEMISTRY VOL. 285, NO. 51, pp. 40312–40321, December 17, 2010

Phosphatidylinositol 3,5-Bisphosphate (PI(3,5)P2) Potentiates Cardiac Contractility via Activation of the Ryanodine Receptor*[S]

Received for publication, August 31, 2010, and in revised form, October 11, 2010 Published, JBC Papers in Press, October 14, 2010, DOI 10.1074/jbc.M110.179689

Chad D. Touchberry[‡], Ian K. Bales[‡], Jessica K. Stone[‡], Travis J. Rohrberg[‡], Nikhil K. Parelkar[‡], Tien Nguyen[‡], Oscar Fuentes[§], Xia Liu[¶], Cheng-Kui Qu[¶], Jon J. Andresen[‡‖], Héctor H. Valdivia[**], Marco Brotto[‡‖], and Michael J. Wacker[‡‖1]

From the Schools of [‡]Medicine and [‖]Nursing, Muscle Biology Research Group, University of Missouri, Kansas City, Missouri 64108, the [§]Departamento de Ciencias Básicas, Universidad del Bío-Bío, 3780000 Chillán, Chile, the [¶]School of Medicine, Case Western Reserve University, Cleveland, Ohio 44106, and the [**]School of Medicine and Public Health, University of Wisconsin, Madison, Wisconsin 53711

Phosphatidylinositol 3,5-bisphosphate (PI(3,5)P2) is the most recently identified phosphoinositide, and its functions have yet to be fully elucidated. Recently, members of our muscle group have shown that PI(3,5)P2 plays an important role in skeletal muscle function by altering Ca^{2+} homeostasis. Therefore, we hypothesized that PI(3,5)P2 may also modulate cardiac muscle contractility by altering intracellular Ca^{2+} ($[Ca^{2+}]_i$) in cardiac myocytes. We first confirmed that PI(3,5)P2 was present and increased by insulin treatment of cardiomyocytes via immunohistochemistry. To examine the acute effects of PI(3,5)P2 treatment, electrically paced left ventricular muscle strips were incubated with PI(3,5)P2. Treatment with PI(3,5)P2 increased the magnitude of isometric force, the rate of force development, and the area associated with the contractile waveforms. These enhanced contractile responses were also observed in MIP/*Mtmr14*$^{-/-}$ mouse hearts, which we found to have elevated levels of PI(3,5)P2. In cardiac myocytes loaded with fura-2, PI(3,5)P2 produced a robust elevation in $[Ca^{2+}]_i$. The PI(3,5)P2-induced elevation of $[Ca^{2+}]_i$ was not present in conditions free of extracellular Ca^{2+} and was completely blocked by ryanodine. We investigated whether the phosphoinositide acted directly with the Ca^{2+} release channels of the sarcoplasmic reticulum (ryanodine receptors; RyR2). PI(3,5)P2 increased [^{3}H]ryanodine binding and increased the open probability (P_o) of single RyR2 channels reconstituted in lipid bilayers. This strongly suggests that the phosphoinositide binds directly to the RyR2 channel. Thus, we provide inaugural evidence that PI(3,5)P2 is a powerful activator of sarcoplasmic reticulum Ca^{2+} release and thereby modulates cardiac contractility.

Phosphatidylinositols are negatively charged amphiphilic phospholipids that are integral members of the lipid bilayer (1). These phosphatidylinositols are concentrated on the cytosolic and sarcoplasmic reticulum (SR)[2] surfaces (2, 3) of cell membranes and are differentially phosphorylated at the 3, 4, and 5 positions of the inositol ring, thereby allowing for the formation of seven distinct phospholipids called phosphoinositides (PIs) (1, 4). Phosphoinositides are uniquely able to undergo rapid and reversible phosphorylation, which is an attribute that makes them ideal membrane signaling proteins. The broadness of cellular functions controlled and modulated by PIs seems to be growing. The significance of PIs is underscored by the growing number of diseases associated with altered PI metabolism such as X-linked myotubular myopathy, Charcot-Marie-Tooth disease, diabetes, and others (5).

The most recently identified PI, phosphatidylinositol 3,5-bisphosphate (PI(3,5)P2), which is regulated by the enzyme muscle-specific inositol phosphatase/myotubularin-related protein 14 (MIP/*Mtmr14*), is essential for maintaining Ca^{2+} homeostasis in skeletal muscle (3). Interestingly, MIP$^{-/-}$ mice have elevated levels of PI(3,5)P2 in skeletal muscle and show significant impairment of skeletal muscle function including: reduced tolerance to treadmill running, increased exercise-induced fatigability, and premature muscle atrophy (3). The reduced skeletal muscle function of MIP$^{-/-}$ mice was attributed to the chronic leakage of Ca^{2+} from the sarcoplasmic reticulum due to direct binding of PI(3,5)P2 to the skeletal muscle ryanodine receptor (RyR1). These data strongly suggest that chronic PI(3,5)P2 dysregulation may be associated with dysfunctional Ca^{2+} handling and impaired contractile performance. However, the role of PI(3,5)P2 in cardiac muscle and its potential contribution to cardiovascular disease are currently unknown.

The regulatory processes that allow for proper functioning of the excitation-contraction coupling (ECC) process in cardiac muscle are highly complex and differ from skeletal muscle in many aspects. In cardiac muscle, ECC regulation is complicated by the fact that Ca^{2+} entry across the sarcolemma via voltage-gated Ca^{2+} channels directly triggers Ca^{2+} release from the SR Ca^{2+} release channels (ryanodine recep-

* This work was supported, in whole or in part, by National Institutes of Health Grant 1RC2AR058962-0110 from the NIAMS (to M. B., J. J. A., and M. J. W.) and ROI-HL055438 (to H. H. V.) from the H. L. B. I. This work was also supported by Missouri Life Sciences Research Board Grant 09-1101 (to M. B., J. J. A., and M. J. W.), an American Heart Association grant (to M. B. and J. J. A.), and a DIPRODE-UBB grant (to O. F.).

[S] The on-line version of this article (available at http://www.jbc.org) contains supplemental Figs. S1–S3.

[1] To whom correspondence should be addressed: 2464 Charlotte St, Kansas City, MO 64108. Tel.: 816-235-6069; Fax: 816-235-6517; E-mail: wackerm@umkc.edu.

[2] The abbreviations used are: SR, sarcoplasmic reticulum; PI(3,5)P2, phosphatidylinositol 3,5-bisphosphate; PI(4,5)P2, phosphatidylinositol 4,5-bisphosphate; PI(3)P2, phosphatidylinositol 3-bisphosphate; PIP, phosphatidylinositol 4-monophosphate; MIP, muscle-specific inositol phosphatase; RyR, ryanodine receptor; ECC, excitation-contraction coupling; CICR, Ca^{2+}-induced Ca^{2+} release.

tors) in a process known as Ca^{2+}-induced Ca^{2+} release (CICR). It is precisely this augmentation in Ca^{2+} release from the cardiac ryanodine receptors (RyR2) that allows for adjustments in cardiac contractility. Despite the significant progress made in the last decade, there is still not a thorough understanding of all the mechanisms that regulate intracellular Ca^{2+} ($[Ca^{2+}]_i$) and subsequent muscle contraction. We hypothesized that PI(3,5)P2 could serve as a novel mechanism to regulate Ca^{2+} and cardiac muscle contractility.

Importantly, it has been shown that PI(3,5)P2 levels can be acutely increased in the cell by hormonal control (6) and environmental stress (7, 8). Few data are available on what effects this increase in PI(3,5)P2 has on cardiomyocytes. It is known that the MIP enzyme is highly expressed in cardiac tissue (3); however, the presence of PI(3,5)P2 in cardiac muscle has remained unreported. Based on the available literature, we wanted to determine whether PI(3,5)P2 was present in cardiomyocytes and explore its role in altering cardiac function. We hypothesized that exogenous PI(3,5)P2 would increase cardiac contractility via direct actions on the cardiac ryanodine receptor (RyR2), which could increase cytosolic Ca^{2+} release. Moreover, we sought to address the physiological role of elevated levels of endogenous PI(3,5)P2 by using $MIP^{-/-}$ mice. We hypothesized that $MIP^{-/-}$ animals would also demonstrate altered cardiac function.

EXPERIMENTAL PROCEDURES

Materials—The PIs, the carrier protein histone H1, and the PI(3,5)P2 antibody were purchased from Echelon Biosciences (Salt Lake City, UT). PBS, Hanks' balanced salt solution, Triton X-100, and fura-2 were obtained from Invitrogen. The secondary antibody light goat anti-mouse IgG2b and the AffiniPure® Fab fragment goat-anti mouse IgG (H+L) (used in the blocking buffer) were obtained from Jackson ImmunoResearch (West Grove, PA). The adult rat/mouse cardiomyocyte isolation kit (ac-7018) was acquired from Cellutron Life Technology (Baltimore, MD). 4, 6-Diamidino-2-phenylindole (DAPI) was purchased from Sigma. Ryanodine was obtained from Ascent Scientific (Princeton, NJ). All remaining reagents were purchased from Fisher Scientific.

Statistical Analysis—All graphs were made and statistical procedures were performed using GraphPad Prism 5.0. Data are presented as means ± S.E. Data were compared using either a paired *t* test or a one-way analysis of variance, and significance was set at the $p < 0.05$ level. When necessary, the one-way analysis of variance was followed up by appropriate post hoc testing. Specific details of the statistical tests performed are stated in the corresponding sections below.

Experimental Animals—Sixteen-week- and 1-year-old wild type male C57/BL6 mice (Jackson Laboratories) and 1-year-old $MIP^{-/-}$ mice (as described previously) (3) were used in this study. All mice were housed in a temperature-controlled (22 ± 2 °C) room with a 12-h:12-h light/dark cycle. Animals were fed *ad libitum*. All protocols were approved by the Animal Care and Use Committee of the University Missouri-Kansas City School of Medicine. Prior to use, mice were treated with heparin (5000 units/kg of body weight) by intraperitoneal injection 30 min before cervical dislocation.

Phosphoinositides—Aqueous stocks (1 mM) of long chain di-C16 fatty acid PIs were prepared in Ringer's solution with Ca^{2+} (in mM: 142 NaCl, 5.0 KCl, 2.5 $CaCl_2$, 1.8 $MgCl_2$, 5 HEPES, 10 glucose, pH 7.4) or without Ca^{2+} (in mM: 142 NaCl, 5.0 KCl, 0.1 EGTA, 2.0 $MgCl_2$, 5 HEPES, 10 glucose, pH 7.4). Because the PIs used are hydrophobic, they were mixed by heating and sonication for 30 min prior to being at stored at −20 °C. These PI stocks were thawed, sonicated, and then vortexed in a (1.0/0.8 ratio) with a carrier solution containing histone H1 to aid in delivering the PIs into the cell. Vehicle experiments were performed using only the histone carrier. The final concentrations of PIs (0.5 μM) and histone carrier (0.4 μM) for contractility and cell culture experiments were determined following preliminary studies and were based off of previous publications (3, 9, 10). Lastly cardiomyocytes were exposed to PI(3,5)P2 (0.5 μM) for 4 h and then underwent a trypan blue dye exclusion assay. No toxic effect was observed to the cardiomyocytes as a result of PI(3,5)P2 or the histone carrier.

Culture of HL-1 Cardiomyocytes—The HL-1 cell line was a kind gift from Dr. W. C. Claycomb (Louisiana State University Health Science Center, New Orleans, LA). HL-1 cells are currently the only cardiomyocyte cell line available that will continuously divide and spontaneously contract while maintaining a differentiated cardiac phenotype (supplemental Fig. S1). Extensive characterization of HL-1 cells via microscopy, genetics, electrophysiological, and pharmacological techniques has demonstrated that HL-1 cells behave similarly to mouse primary cardiomyocytes (11), which are difficult to obtain and maintain in prolonged culture. Cells were cultured in T-25 flasks precoated with a 0.00125% fibronectin and 0.02% gelatin solution and maintained in Claycomb medium (JRH Biosciences Ltd.) supplemented with 10% fetal bovine serum, 2 mM L-glutamine, 0.1 mM norepinephrine, 0.3 mM ascorbic acid, and 100 units/ml penicillin, 100 mg/ml streptomycin (full media), at 37 °C in a humid atmosphere of 5% CO_2, 95% air. Media were changed every 24–48 h. For experiments, cells were seeded at 3500 cells/35-mm dish and allowed to recover for 24 h prior to experimentation. HL-1 cells (supplemental Fig. S1) were tested with PI(3,5)P2 and histone carrier, in the presence of extracellular Ca^{2+} (1.8 mM), in the absence of extracellular Ca^{2+} (0.0 mM), and with ryanodine (1 μm) in the presence of Ca^{2+}. This dose of ryanodine was chosen as it inhibited the response of the SR to caffeine (10 mM).

Isolation of Primary Cardiac Myocytes—To confirm the results demonstrated in our stable HL-1 cell line, we repeated essential experiments in adult primary cardiac myocytes. Primary cardiac myocytes were isolated using the non-perfusion adult rat/mouse cardiomyocyte isolation kit, which yields ~20% healthy, viable myocytes in our laboratory (supplemental Fig. S1). Briefly, the tissue was cut vertically into small pieces with a pair of scissors. The pieces were then transferred into a 50-ml tube and digested at 37 °C on a shaker at the speed of 85–100 rpm. Repeated cell suspensions were collected (4–6 times), and cells were centrifuged (250 × *g*) for 2 min, rinsed in wash buffer, and transferred to laminin-treated plates. The isolated cardiac myocytes underwent a 2-h incubation at 37 °C to allow the cells to attach to the plate. Pri-

mary cells were tested with PI(3,5)P2 and histone carrier, in the presence of Ca^{2+} (1.8 mM), and with ryanodine (0.1 μm). This dose of ryanodine was chosen as it inhibited the response of the SR to caffeine (10 mM) in primary myocytes.

Immunochemistry—Following cervical dislocation, whole hearts were quickly excised, rinsed in PBS, and frozen until use. Hearts were later embedded in tissue freezing medium and sectioned at 8 μm using a cryostat. Immunohistochemistry was then performed as described previously (12). Briefly, sections were mounted to a slide and fixed in 4% formaldehyde for 10 min at room temperature. Slides were washed with 0.5% Triton X-100 in TBS followed by blocking with 10% normal goat serum. Sections were incubated overnight at 4 °C with either anti-PI(3,5)P_2 mouse monoclonal IgG2b antibody (1:500) in blocking buffer. On the second day, sections were allowed to incubate at room temperature for 1 h followed by three washes in TBS for 5 min each. This was followed by incubation with a fluorescently tagged DyLight goat anti-mouse IgG2b specific secondary antibody (1:5000) in blocking buffer for 1 h at room temperature. Following this, sections were incubated with DAPI, 1 μg/ml in blocking buffer for 5 min. Prior to being coverslipped, sections were washed three times in TBS. Sections were dried and coverslipped with mounting medium. Negative control sections (non-immune) were performed by incubating with antibody diluent and DAPI stain and supplementing with a non-immune immunoglobulin of the same isotype as the primary antibody (supplemental Fig. S2).

To test for changes in the levels of endogenous PI(3,5)P2 HL-1 cells were grown on coverslips and serum-starved overnight in Claycomb minimal media (0.5% fetal bovine serum, 2 mM L-glutamine, and 100 units/ml penicillin, 100 mg/ml streptomycin). Cells were then rinsed with TBS and transferred into serum-free DMEM (2 mM L-glutamine, 100 units/ml penicillin, and 100 mg/ml streptomycin) for 4 h. The switch from Claycomb media to DMEM was essential as the Claycomb media contains insulin and other growth factors (11). After 4 h, the cells were given fresh serum-free DMEM and treated with insulin (1 milliunit/ml) for 10 min. Immunocytochemistry was then performed as described above.

Fluorescent images were captured with an Olympus IX51 inverted microscope (Center Valley, PA), Hamamatsu Orca-ERGA CCD camera (Bridgewater, NJ), Semrock BrightLine filter set (Rochester, NY), and X-cite 120 metal halide light source (EXFO, Mississauga, CA). Data were captured and analyzed with the SlideBook ratiometric software (Intelligent Imaging Innovations Inc., Denver, CO). Differences in the relative immunofluorescence between groups was detected using a paired *t* test. Experiments were repeated three times to confirm results.

Cardiac Contractility Measurements—The mouse hearts used for the muscle strip experiments were quickly excised and placed into an ice-cold cardioprotective Ringer's solution (with Ca^{2+}) that included the addition of 2,3-butanedione monoxime (30 mM) and insulin (10 IU/liter) for 30 min, bubbled under 100% O_2 as described previously (13). Briefly, left ventricular muscle strips were prepared (1–2 mm wide by 6–8 mm long) in the cardioprotective solution. The strips were tied on the proximal and distal ends with a silk thread. The muscle strips were then rinsed three times (5 min each) in Ringer's (with Ca^{2+}, pH, 7.4) to remove the 2,3-butanedione monoxime. Cutting the ventricles into strips exposes a greater surface area of the heart to the PIs and was essential for PI delivery.

In $MIP^{-/-}$ contractility experiments, we utilized intact ventricular tissue. Hearts were isolated and placed into ice-cold Ringers solution (with Ca^{2+}), and atria were removed. Hearts were attached to silk thread using small metallic clips.

The muscle strips and intact hearts were hung vertically and attached to force transducer, between bipolar platinum stimulating electrodes suspended in 25-ml glass tissue chambers, all of which were obtained from AD Instruments (Colorado Springs, CO). Heart muscles were stretched to the length of maximum force development in Ringer's solution (pH, 7.4, without 2,3-butanedione monoxime) and stimulated with pulses of 1 Hz for 5 ms (Grass Technologies stimulator SD9; Quincy, MA) the voltage was set 20% above threshold. The muscles in the chamber were superfused with Ringer's solution (with Ca^{2+}, pH, 7.4) continuously bubbled with 100% O_2 at room temperature. Muscles were allowed to stabilize for 90 min prior to experimentation and provided with fresh media changes every 30 min. Muscles were paced at 1 Hz to obtain a stable baseline and were drug-treated with either vehicle (histone) or PIPs. The contractile data were recorded and analyzed on the LabChart 6 software; AD Instruments (Colorado Springs, CO). Waveform changes were analyzed in the segments corresponding to peak isometric tension (millinewtons). Slope (millinewtons/s) was analyzed by taking the average slope from 10 to 20 ms after the start of the peak. Area (millinewtons $\times$ s) was calculated using the region from 10 to 90% of the peak. τ (s) was fitted at the baseline using data from 95 to 0% of peak. For exogenous PI experiments, three heart strips were tested in two different PIs and compared with a histone only vehicle control. Each group therefore represents muscle strips from 5 to 6 different animals. Strip experiments were normalized within each condition to baseline levels of contractility and presented as a relative change from baseline contraction data. Differences for isometric tension were analyzed by a one-way analysis of variance followed with a Newman-Keuls multiple comparison post hoc test. Differences for slope, area, and τ were analyzed via a paired *t* test.

The intact ventricular experiments of $MIP^{-/-}$ animals were compared with age-matched WT controls. The tension data for the intact experiments were taken during the maximal contraction evoked by electrical stimulation at 1 Hz. The isometric tension was normalized to heart weight and is presented as relative force. Differences for isometric tension, slope, area, and τ were analyzed by a paired *t* test.

Ca^{2+} Imaging—Imaging was conducted as reported previously (14). Briefly, all cells were loaded with the Ca^{2+} indicator fura-2 (2 μM) for 30 min at 37 °C and allowed to de-esterify for 10 min at 37 °C. Plates were washed twice with Hanks' balanced salt solution, and intracellular Ca^{2+} levels were measured at 37 °C using an environmental chamber. Data were captured and analyzed with the SlideBook ratiometric software. Cell culture dishes were pretreated with ryanodine

for 10 min prior to treatment with PI(3,5)P2. Primary cells were treated with KCl (80 mM) to determine viability at the end of each test. All diluted drugs were added by dilute bolus injection on the plates. Cells for imaging were selected on the distal side of the plate to allow for drug dilution and diffusion. Nevertheless, because cells may not be equal distances from the drug delivery site, this may contribute to some variability in cell responses. In these experiments, the three treatment conditions (vehicle, PI(3,5)P2 alone, or PI(3,5)P2 + ryanodine) were tested 2–3 times each from isolated cardiac myocytes from a given animal (6–9 cells). The experiments were repeated in five animals, and therefore, a total of 10–15 primary cardiac myocytes were tested for each treatment condition. All data are presented at the peak increase in fluorescence. The cells tested in each condition were averaged and then used for data analysis. Data were analyzed by a one-way analysis of variance followed by Newman-Keuls multiple comparison post hoc test.

[^{3}H]Ryanodine Binding Assay—[^{3}H]Ryanodine binding to purified pig cardiac muscle SR was performed as described previously (15, 16). The standard incubation medium (0.2 M KCl, 40 mM Na-HEPES at pH 7.2, 7 nM [^{3}H]ryanodine, 1 mM EGTA) contained $CaCl_2$ in amounts necessary to set free [Ca^{2+}] between 10 nM and 10 mM. Samples (0.1 ml) were run in duplicate and incubated at 37 °C for 90 min. The Ca^{2+}/EGTA ratio was calculated by using the online software program MaxChelator. Cardiac muscle SR-enriched microsomes (60 μg) were added to the incubation medium together with 10 μM PI(3,5)P2. Nonspecific [^{3}H]ryanodine binding was determined in the presence of unlabeled ryanodine (10 μM), amounted typically to no more than 10–15%, and was subtracted from all reported values.

Planar Lipid Bilayer Technique—SR-enriched microsomes from pig heart were reconstituted into Muller-Rudin planar lipid bilayers as described previously (15, 16). Control and PI(3,5)P2 were run using the same vesicles; therefore, the density of RyR2 was the same in each condition. Single RyR2 channel data were collected at steady voltages (+35 mV, *cis* chamber grounded) for 2 min in symmetrical cesium methane-sulfonate (300 mM) and Na-HEPES (10 mM at pH 7.2). The recording solution contained ~5 μM free Ca^{2+} as assessed by a calibration curve, which was sufficient to activate the RyR2 channel. EGTA (1 mM), and a calibrated concentration of $CaCl_2$ was then added to the *cis* (cytosolic) side of the channel to reach a free [Ca^{2+}] in the range of *p*Ca 7 to *p*Ca 4. After recording RyR2 channel activity in the absence of PI(3,5)P2, the PI or vehicle was added to the cytosolic side of the channel. For each condition, single channel data were collected at steady voltages for 2–5 min. The bilayer was "rested" at 0 mV to improve stability while adding reagents or perfusing the *cis* chamber. Channel activity was recorded with a 16-bit VCR-based acquisition and storage system at a 10-kHz sampling rate. Signals were analyzed after filtering with an 8-pole Bessel filter at a sampling frequency of 1.5–2 kHz. Data acquisition and analysis were done with Axon Instruments software and hardware (pCLAMP v9, Digidata 200 AD/DA interface). Cationic inward currents are represented by upward deflections of the baseline current (17). The mean duration and amplitude of open events were defined by two threshold detectors placed between the baseline and the mean open current. One detector was placed 1 S.D. above the mean of the baseline current, and the second detector was placed at 1 S.D. below the mean current of the open channel. Open and close time intervals were obtained from idealized records. Dwell time distributions were logarithmically binned with equally spaced time intervals (6–8 bins/decade) and fitted to probability density functions by the maximum likelihood method (correlation coefficients > 0. 96). Data on open probability of the RyR channel were analyzed using a paired *t* test.

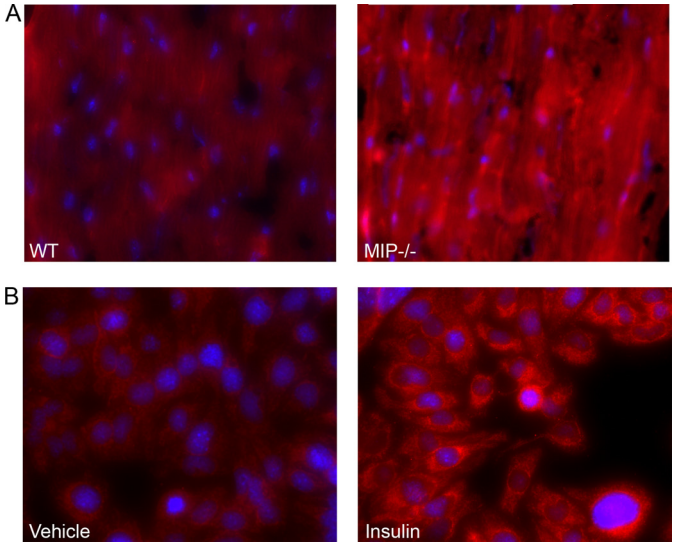

FIGURE 1. **PI(3,5)P2 is present in WT mice, elevated in MIP$^{-/-}$ mice, and modulated by insulin in cardiac myocytes.** *A* shows the immune cross-section, which was probed with DAPI (*blue*) and a primary antibody for PI(3,5)P2 (*red*) comparing WT with MIP$^{-/-}$ heart sections. *B* shows HL-1 cardiomyocytes, which were treated with DAPI (*blue*) and a primary antibody for PI(3,5)P2 (*red*) but not treated with insulin. HL-1 cells underwent immunocytochemistry 10 min following incubation with insulin (1 milliunit/ml) (n = 50–100 cells/experiment). Wild type *versus* MIP$^{-/-}$ and Vehicle *versus* Insulin sections were set at the same fluorescent values for any pixel and below the saturation limit of the camera (4096). Images were captured with a 40× objective.

RESULTS

Immunohistochemistry—To determine a potential physiological role for PI(3,5)P2, we first determined its presence in cardiac tissue. Fig. 1*A* shows wild type and MIP$^{-/-}$ mouse ventricular cross-sections, which were stained with DAPI and PI(3,5)P2 antibody. MIP$^{-/-}$ animals (2.70 ± 0.17) showed increased immunofluorescence over wild type controls (2.15 ± 0.03).

Moreover, we observed an increase in PI(3,5)P2 immunofluorescence following insulin treatment of HL-1 cells (0.54 ± 0.15) over non-insulin-treated controls (0.27 ± 0.06) (Fig. 1*B*). These immunocytochemistry results clearly demonstrate that PI(3,5)P2 is present and responsive to physiological challenges in cardiomyocytes.

Contractility—Our next aim was to elucidate the effect of exogenous PI(3,5)P2 in cardiac muscle contractility. We compared the contractile responses elicited by PI(3,5)P2 with the isomer PI(4,5)P2, as well as the phosphatase-reduced form of PI(3,5)P2 known as PI(3)P (Fig. 2). Peak changes in PIPs were

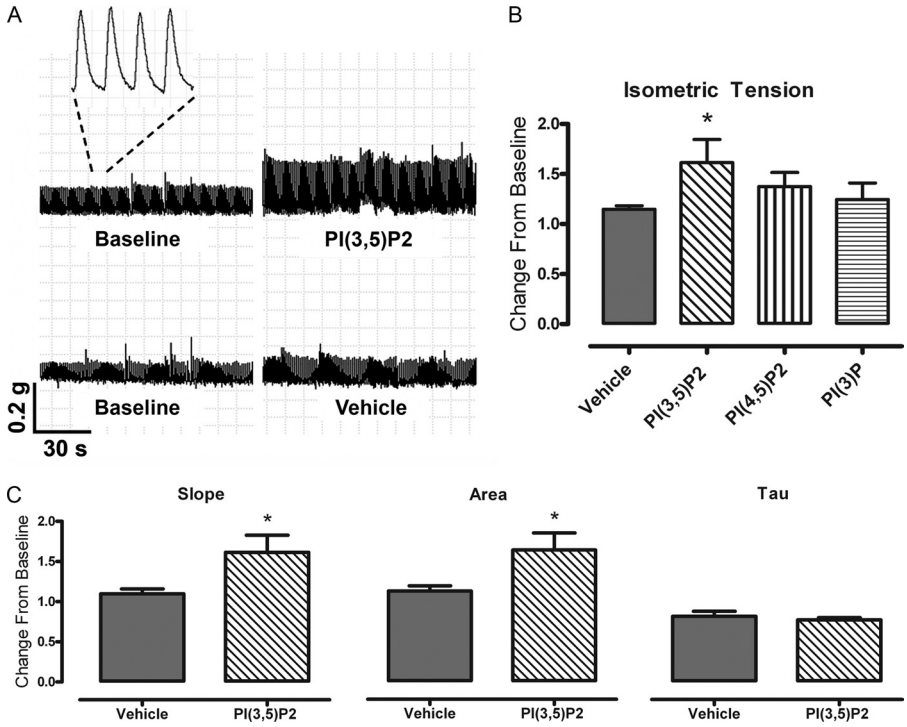

FIGURE 2. **PI(3,5)P2 acutely increases contractile force in *ex vivo* ventricular cardiac muscle strips.** *A* contains representative tracings of left ventricular muscle contractions at baseline and following treatment with either PI(3,5)P2 or vehicle. *B* summarizes isometric tension data and shows that PI(3,5)P2 increased tension, whereas PI(4,5)P2 and PI(3)P did not elicit a significant response when compared with vehicle. *C* shows that PI(3,5)P2 increased the slope and area, but not τ ($n = 4$–5 animals). * denotes statistical significance from vehicle.

noted between 25 and 35 min following treatment. Fig. 2*A* displays the raw tracings of a ventricular muscle strip to PI(3,5)P2 and histone. PI(3,5)P2 (0.5 μM; $n = 5$ animals) increased isometric force on average (1.61 ± 0.23) when compared with vehicle (1.15 ± 0.03) (Fig. 2*B*), whereas treatment of muscle strips with PI(4,5)P2 (0.5 μM; $n = 5$ animals) and PI(3)P (0.5 μM; $n = 5$ animals) did not increase isometric force development when compared with vehicle (1.36 ± 0.14 and 1.25 ± 0.17, respectively) (Fig. 2*B*). Next, we analyzed the effects of PI(3,5)P2 on specific characteristics of each contractile waveform. PI(3,5)P2 increased the slope of contraction (1.61 ± 0.21) when compared with vehicle (1.10 ± 0.06). Further, PI(3,5)P2 also increased the overall area of the contractile waveform (*i.e.* the integral) (1.65 ± 0.21) when compared with vehicle (1.13 ± 0.06). PI(3,5)P2, however, had no effect on τ, the time constant of decay (rate of relaxation) (0.96 ± 0.03), when compared with vehicle (1.02 ± 0.08) (Fig. 2*C*).

Next, we tested the role of endogenous PI(3,5)P2 in cardiac muscle contractility using $MIP^{-/-}$ animals. We compared the contractile responses elicited by $MIP^{-/-}$ with the wild type age-matched controls (Fig. 3). Fig. 3*A* displays a sample contraction during maximal stimulation from a WT and $MIP^{-/-}$ contractility experiment. Similar to what we found with exogenous PI(3,5)P2, cardiac muscles from $MIP^{-/-}$ animals ($n = 4$) demonstrated an increased relative-isometric force (63.00 ± 17.76) when compared with wild type (34.75 ± 8.59) (Fig. 3*B*). Next, we analyzed the specific characteristics of each contractile waveform between $MIP^{-/-}$ and wild type animals. $MIP^{-/-}$ animals had increased slope of contraction (89.50 ± 26.62) when compared with wild type (50.00 ± 14.28) and also an increase in the overall area of the contractile waveform (*i.e.* the integral) (2.88 ± 0.69) when compared with the wild type controls (1.30 ± 0.31). $MIP^{-/-}$ mice, however, had no effect on τ (0.10 ± 0.01) when compared with wild type animals (0.10 ± 0.01) (Fig. 3*C*).

Ca^{2+} Imaging of HL-1 Cardiomyocytes—The contractile data indicated that PI(3,5)P2 acts in cardiac muscle by altering intercellular Ca^{2+} homeostasis. To test whether the source of Ca^{2+} was from an intracellular or extracellular source, we tested the response of HL-1 cells loaded with the Ca^{2+} indicator fura-2 to PI(3,5)P2 in the absence and presence of Ca^{2+} (1.8 mM). Fig. 4*A* shows a raw trace of the ratiometric change in $[Ca^{2+}]_i$ measured in HL-1 cardiac myocytes before and after exposure to PI(3,5)P2. Fig. 4*B* shows the average ratiometric change in intracellular Ca^{2+} at baseline and following exposure to PI(3,5)P2. Treatment of HL-1 cells tested in extracellular Ca^{2+} with PI(3,5)P2 elevated the peak cytosolic Ca^{2+} (1.68 ± 0.33) over vehicle (0.64 ± 0.02). There was no difference in the peak ratiometric response to PI(3,5)P2 between tests performed in the presence (1.68 ± 0.33) or absence (1.61 ± 0.32) of extracellular Ca^{2+}. To test the involvement of the cardiac RyR2 channel, we pretreated HL-1 cells with ryanodine (Fig. 4*B*). Following pretreatment with ryanodine, the myocytes were treated with PI(3,5)P2, and the response was significantly reduced. Blockade of the SR by ryanodine inhibited the effect of PI(3,5)P2 (0.65 ± 0.06) and showed no statistical difference when compared with vehicle (0.64 ± 0.02). The baseline data represent the average ratiometric value prior to any treatment. Vehicle treatment was

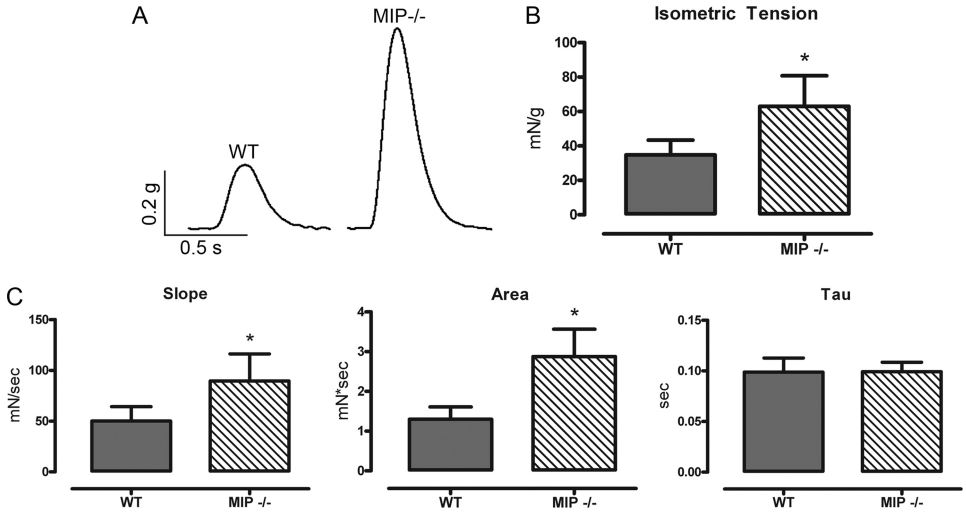

FIGURE 3. **$MIP^{-/-}$ mice show increased contractile force in *ex vivo* intact ventricular cardiac muscle.** *A* shows a raw tracing of a ventricular muscle contraction from a $MIP^{-/-}$ mouse and an age-matched WT mouse. *B* summarizes isometric tension data and shows that $MIP^{-/-}$ mice had increased isometric tension when compared with WT age-matched controls. *mN*, millinewtons. *C* presents the averages showing that $MIP^{-/-}$ mice have an increased slope and area, but not τ ($n = 4$). * denotes statistical significance from wild type age-matched controls.

included as a comparison with baseline and demonstrates that the histone carrier had no effect on $[Ca^{2+}]_i$. The average time for a response to PI(3,5)P2 was 140 ± 41 s for PI(3,5)P2.

Ca^{2+} Imaging of Isolated Primary Cardiac Myocytes—Next, we wanted to confirm our finding that the effects of PI(3,5)P2 were mediated by the RyR2 channel in primary cardiomyocytes. Fig. 5*A* shows a raw trace of the ratiometric change in intracellular Ca^{2+} measured in a primary ventricular cardiac myocyte before and after exposure to PI(3,5)P2. Treatment with PI(3,5)P2 elevated the Ca^{2+} level, which typically remained elevated for several minutes, eventually causing contraction of the myocyte. To reaffirm that exposure to PI(3,5)P2 acts principally on the RyR2 channel, we pretreated primary cardiac myocytes with ryanodine. Fig. 5*B* shows that the normal caffeine-evoked ratiometric Ca^{2+} response is effectively blocked following treatment of primary cardiac myocytes with ryanodine, indicating that the SR Ca^{2+} pool was disabled. Following pretreatment with ryanodine, the primary cardiac myocytes were treated with PI(3,5)P2, and the response was significantly reduced. Lastly the primary cardiac myocytes were given KCl (80 mM) to ensure viability of the cell. Fig. 5*C* shows average ratiometric fura-2 responses at baseline, vehicle treatment, PI(3,5)P2 treatment, and pretreatment with ryanodine. Treatment of primary cardiac myocytes tested in extracellular Ca^{2+} with PI(3,5)P2 elevated the cytosolic Ca^{2+} (1.53 ± 0.13) when compared with vehicle (0.40 ± 0.06). Blockade of the SR with ryanodine significantly inhibited the effect of PI(3,5)P2 (0.51 ± 0.05) and showed no statistical difference when compared with vehicle. The average time for a response to PI(3,5)P2 was 161 ± 68 s.

[^{3}H]Ryanodine Binding and RyR2 Channel Activity—To test the hypothesis that PI(3,5)P2 triggers SR Ca^{2+} release by activation of RyR2, we used a [^{3}H]ryanodine binding assay. Because [^{3}H]ryanodine binds only to the open conformational state of the channel, binding of the alkaloid is proportional to the activity of the channel (15, 16). Fig. 6*A* shows that PI(3,5)P2 increased [^{3}H]ryanodine binding to cardiac SR preps over a wide range (0.01 μM–0.01 mM) of $[Ca^{2+}]$, but the effect was very pronounced at the lower Ca^{2+} concentrations (100 nM and 1 μM). This PI(3,5)P2 sensitization of the RyR2 is specific as the effect was significantly inhibited by a PI(3,5)P2 antibody (supplemental Fig. S3) and is concentration-dependent, with maximal stimulation (B_{max}) = 308 ± 22% and half-maximal effective dose (ED_{50}) = 6.2 ± 1.2 μM ($n = 4$ experiments) (Fig. 6*B*). To test whether [^{3}H]ryanodine binding results indeed correlated with RyR2 channel activity, we reconstituted cardiac SR vesicles in planar lipid bilayers and recorded RyR2 channel activity in the absence and presence of PI(3,5)P2. Several biophysical and pharmacological properties of the recorded channel indicated to us that the activity indeed corresponded to RyR2 channels: 1) the unitary conductance corresponded to ~700 picosiemens, which is typical for RyR2 channels; 2) Ca^{2+} (100 nM-10 μM) in the cytosolic side of the channel increased channel activity; chelation of Ca^{2+} with EGTA decreased channel activity; 3) channels entered into a subconductance state (~40% of full conductance) upon the addition of 100 nM ryanodine, which is a signature effect of the alkaloid on RyR channels. Under control conditions and at 100 nM free $[Ca^{2+}]$ (*p*Ca 7), RyR2 channel activity was low (open probability, P_o, ≤ 0.05), as expected, but increased dramatically upon the addition of PI(3,5)P2 to the cytosolic side of the channel (Fig. 7*A*). The activity increased by 471% with respect to control, with nP_o (single channel P_o multiplied by the number of observed channels) increasing from 0.03 ± 0.02 in control to 0.18 ± 0.06 after PI(3,5)P2 ($n = 6$ experiments) (Fig. 7*B*). A dramatic increase in P_o was detected immediately after the addition of PI(3,5)P2 to the cytosolic side of the channel as seen in the P_o *versus* time plot (Fig. 7*C*). The effect of PI(3,5)P2 lasted more than the mean life of the bilayers, suggesting a ligand-receptor interaction.

DISCUSSION

This is the first study to examine the acute and chronic effects of PI(3,5)P2 in cardiac myocytes. The major findings of

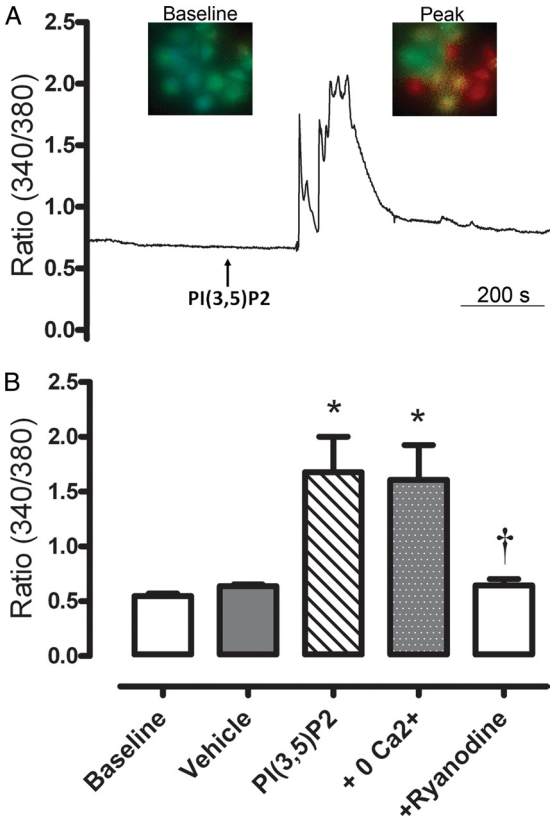

FIGURE 4. **PI(3,5)P2 increases intracellular Ca^{2+} from intracellular stores in HL-1 cardiomyocytes.** *A* shows fura-2 ratiometric changes in intracellular Ca^{2+} in of HL-1 cardiac myocyte after treatment with PI(3,5)P2 in the presence of extracellular Ca^{2+} (1.8 mM). *B* shows the summary of fura-2 ratiometric changes in intracellular Ca^{2+} response in HL-1 cardiomyocytes after exposure to PI(3,5)P2 with extracellular Ca^{2+} (1.8 mM), without extracellular Ca^{2+} (0 mM), and with extracellular Ca^{2+} ryanodine pretreatment. Increases in intracellular Ca^{2+} were not affected by extracellular Ca^{2+} but were fully eliminated by the preaddition of ryanodine ($n = 10–15$ cells/condition). Images were captured with a 40× objective. * denotes statistical significance from vehicle, and † denotes statistical significance from PI(3,5)P2.

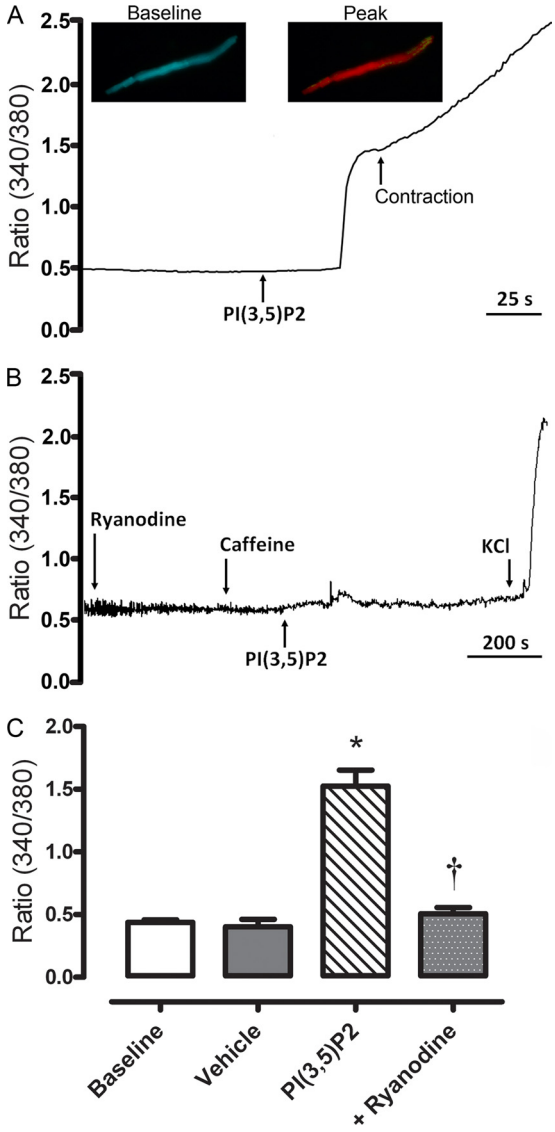

FIGURE 5. **Ryanodine inhibits the elevation of intracellular Ca^{2+} by PI(3,5)P2 in primary cardiac myocytes.** *A* shows fura-2 ratiometric changes in intracellular Ca^{2+} in an isolated ventricular adult cardiac myocyte after treatment with PI(3,5)P2, ultimately resulting in contraction. *B* shows that ryanodine inhibited the release of SR Ca^{2+} to both caffeine and PI(3,5)P2. *C* provides a summary of the data. Results in primary myocytes show that increases in intracellular Ca^{2+} were fully eliminated by the preaddition of ryanodine ($n = 10–15$ cells/condition). Images were captured with a 40× objective. * denotes statistical significance from vehicle, and † denotes statistical significance from PI(3,5)P2.

this study are as follows. 1) PI(3,5)P2 is present and responsive to physiological stress (insulin) in cardiac myocytes; 2) cardiac contractile force, rate of force development, and area (integral) were all increased following exposure to exogenous PI(3,5)P2 and in $MIP^{-/-}$ mice; 3) PI(3,5)P2 binds and increases the open probability of RyR2 channels; and 4) PI(3,5)P2 causes $[Ca^{2+}]_i$ release in cardiac myocytes by acting on RyR2-sensitive Ca^{2+} stores. These findings have led us to propose that PI(3,5)P2 induces increases in cardiac contractility by binding and opening RyR2, which increases the cytoplasmic Ca^{2+} levels needed for the ECC process and stimulation of CICR.

PI(3,5)P2 is a newly identified PI, and its presence in various tissues has yet to be defined. Shen *et al.* (3) have previously shown that the inositol phosphatase, MIP, an enzyme that breaks down PI(3,5)P2, is highly present in both skeletal and cardiac tissue, suggesting that PI(3,5)P2 could potentially be present in the heart. Using immunodetection, we found PI(3,5)P2 expression in longitudinal cross-sections of left ventricular mouse heart. PI(3,5)P2 has previously been shown to be concentrated and localized in the SR of skeletal muscle (3), suggesting that PI(3,5)P2 is in close proximity to, and may modulate, the RyR channels in both cardiac and skeletal muscle.

To investigate the effects of PI(3,5)P2 on cardiac contractility, we compared contractile data in left ventricular muscle strips with those treated with PI(3,5)P2 and vehicle alone. PI(3,5)P2 significantly increased isometric tension, slope, and area of contraction. In addition to PI(3,5)P2, we also tested its isomer, PI(4,5)P2. Recent evidence has suggested that PI(4,5)P2 itself can directly alter ion channel permeability (18). Therefore, we were interested in determining whether this isomer could also induce changes in functional contractile responses. Moreover, we also treated muscle strips with the intermediary product in PI(3,5)P2 synthesis, PI(3)P.

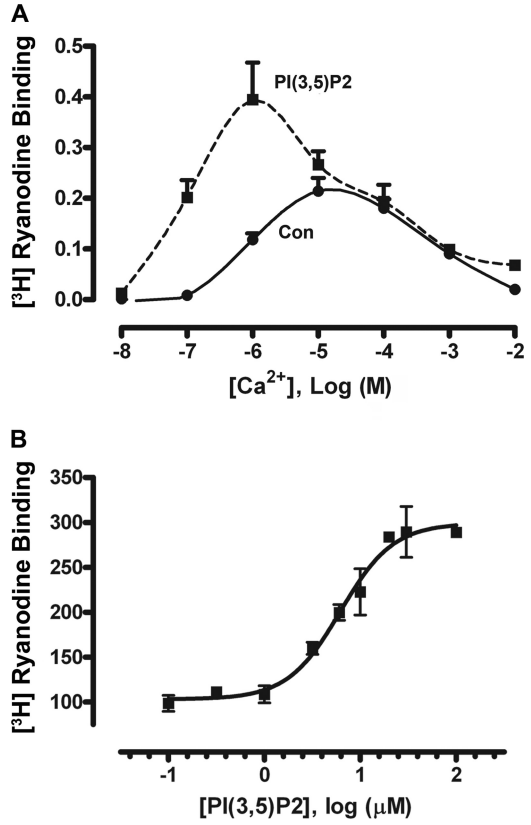

FIGURE 6. **PI(3,5)P2 increases [^{3}H]ryanodine binding to cardiac SR vesicles.** *A* shows the Ca^{2+} dependence of [^{3}H]ryanodine binding to cardiac SR in the absence (*Con*) or presence of PI(3,5)P2 ($n = 4$). *B* is the averaged dose-response curve of PI(3,5)P2 stimulation of [^{3}H]ryanodine binding to cardiac SR. [Ca^{2+}] in the binding medium was "clamped" at *p*Ca 6. Data points were fitted with a Hill function that yielded a maximal stimulation = 308 ± 22% of control (which was determined in the absence of PI(3,5)P2) and half-maximal effective dose (ED_{50}) = 6.2 ± 1.2 μM ($n = 4$). Nonspecific binding (<10% of total binding) was determined with 10 μM ryanodine and subtracted.

Treatment with PI(4,5)P2 and PI(3)P did not alter the characteristics of the contractile waveforms (force, slope, area, and τ) when compared with vehicle. In support of our contractile data, Shen *et al.* (3) found no changes in $[Ca^{2+}]_i$ homeostasis in skeletal muscle fibers treated with PI(4,5)P2 and PI(3)P and concluded that PI(3,5)P2 was the principal mediator of functional changes in skeletal muscles from $MIP^{-/-}$ mice. In our $MIP^{-/-}$ mice, we noted the highly similar changes in cardiac contractility (significantly increased isometric tension, slope, and area of contraction) during maximal stimulation as to those seen with exogenous administration of PI(3,5)P2. These results show that endogenous PI(3,5)P2 has the ability to modulate cardiac contractility. From these contractile data, we hypothesized that the increased contractile force was indicative of an enhanced regulation of $[Ca^{2+}]_i$.

During the cardiac ECC process, force is generated on a beat-to-beat basis by a 10-fold increase in cytosolic Ca^{2+}. As a cardiac myocyte depolarizes, $[Ca^{2+}]_i$ begins to accumulate principally from the opening of L-type Ca^{2+} channels, which triggers CICR from RyR2. In adult mouse myocardium, it is estimated that the RyR2 channel contributes upwards of 70% of the Ca^{2+} ions utilized during contraction and, therefore, it is considered to be the largest determinant of cardiac contractility (19). Because the majority of $[Ca^{2+}]_i$ accumulation during cardiac muscle contraction is from the SR, and PI(3,5)P2 binds and activates RyR1 (3), we hypothesized that PI(3,5)P2 would principally alter the SR Ca^{2+} release from RyR2 in cardiomyocytes.

Our data show that elevated PI(3,5)P2 increased the height, slope, and area of contraction; therefore, it is likely that PI(3,5)P2 improves Ca^{2+} entry either via opening voltage-gated Ca^{2+} channels or via directly altering Ca^{2+} release from RyR2. Moreover, during relaxation, a return to Ca^{2+} homeostasis is controlled principally by the sarcoplasmic reticulum Ca^{2+}-ATPase (sarcoplasmic endoplasmic reticulum Ca^{2+}-ATPase) and the Na^+/Ca^{2+} exchanger, with a very minor contribution by the plasma membrane Ca-ATPase. If PI(3,5)P2 was increasing cytosolic Ca^{2+} and the area of contraction by slowing Ca^{2+} removal, there should be a corresponding increase in τ (the rate of relaxation following contraction). We found that elevated levels of PI(3,5)P2 had no effect on τ, demonstrating that it is very unlikely to have an effect on the activity of sarcoplasmic reticulum Ca^{2+}-ATPase pumps, Na^+/Ca^{2+} exchangers, and/or Ca^{2+} ATPases.

To test the hypothesis that Ca^{2+} was being released principally from the SR, we performed Ca^{2+} imaging on HL-1 cells with or without extracellular Ca^{2+}. HL-1 cells exposed to PI(3,5)P2 showed significant increases in $[Ca^{2+}]_i$. Our data show that the absence of $[Ca^{2+}]_o$ did not affect the magnitude of the $[Ca^{2+}]_i$ response in HL-1 cells exposed to PI(3,5)P2. This strongly suggested that PI(3,5)P2 was not reliant on $[Ca^{2+}]_o$. To test the hypothesis that PI(3,5)P2 was acting on the RyR2 channel to increase Ca^{2+} release from the SR, we explored the inhibitory effect of ryanodine in both HL-1 cells and isolated primary ventricular mouse cardiac myocytes. Importantly, pretreatment with ryanodine eliminated the PI(3,5)P2-induced increase in $[Ca^{2+}]_i$ in both cell types, indicating that PI(3,5)P2 influences SR Ca^{2+} release via RyR2 in cardiomyocytes.

To further test our hypothesis that PI(3,5)P2 regulates Ca^{2+} release via RyR2, we examined the effects of PI(3,5)P2 on [^{3}H]ryanodine binding to RyR2 and with single channel recordings of RyR2 reconstituted in lipid bilayers. We produced a Ca^{2+}-dependent [^{3}H]ryanodine binding curve to determine whether PI(3,5)P2 activates RyR2 at a $[Ca^{2+}]$ similar to that found within myocytes at rest (*p*Ca 7) or during contraction (*p*Ca 6). Because the Ca^{2+} dependence of [^{3}H]ryanodine binding and the open probability (P_o) of RyR2 channels are generally convergent (15, 16), we can correlate [^{3}H]ryanodine binding to RyR2 channel activity. Therefore, [^{3}H]ryanodine binding exhibits a bell-shaped Ca^{2+}-dependent curve, as low $[Ca^{2+}]$ (*p*Ca 8–*p*Ca 6) activates the channel, whereas high $[Ca^{2+}]$ (*p*Ca 4–*p*Ca 2) inactivates the channel. PI(3,5)P2 did not change the bell-shaped form of this curve; however, the ascending limb of the curve was dramatically shifted upward at physiologic levels of Ca^{2+} (*p*Ca 7 and *p*Ca 6). Therefore, PI(3,5)P2 "sensitizes" RyR2s at resting (100 nM) and contractile (1 μM) levels of Ca^{2+}. The "sensitizing" effects of PI(3,5)P2 were blocked in a concentration-dependent manner by the addition of a PI(3,5)P2 antibody.

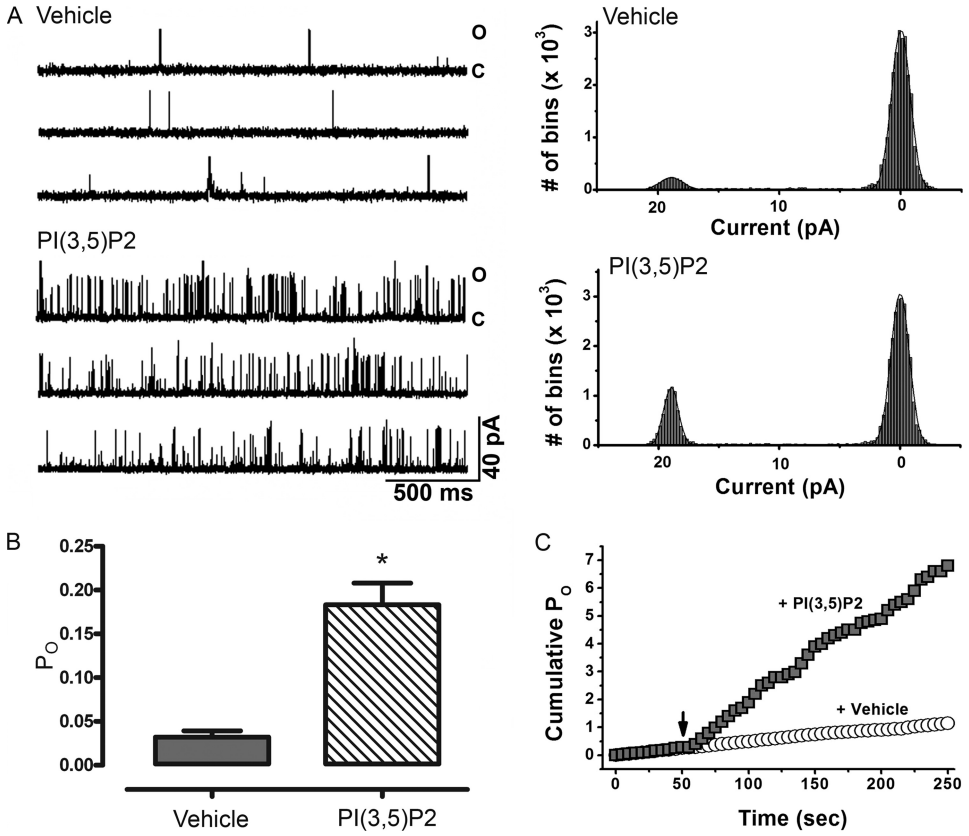

FIGURE 7. **PI(3,5)P2 directly activates RyR2 channels.** SR-embedded RyR2 channels were reconstituted in planar lipid bilayers to test the effect of PI(3,5)P2. *A* shows single channel activity of RyR2 in the absence and the same channel in the presence of PI(3,5)P2. At a cytosolic [Ca^{2+}] = 100 nM (*p*Ca 7), the activity of the channel was low but increased immediately after the addition of PI(3,5)P2 to the cytosolic side. Openings (*o* = open) are shown as upward deflections of the baseline current (*c* = closed). To the *right* are the current amplitude histograms for the channels represented in this panel. The peak at ~20 pA represents the channel in the fully open state, whereas the baseline current (closed channel) peaks at 0 pA. In *B*, the P_o of each RyR2 channel was computed from at least 3 min of activity before and after the addition of PI(3,5)P2. The figure represents the summary of experiments (*n* = 6) and indicates the change of activity before and after the addition of PI(3,5)P2. * denotes statistical significance from control. *C* shows a representative time course of PI(3,5)P2 effect on RyR2 channels. The P_o of a 5-s segment of RyR2 channel activity has been added to the P_o of the previous segment and plotted cumulatively over time. The *arrow* indicates the time in which PI(3,5)P2 or vehicle was added to the cytosolic side of the channel.

To further investigate the effect of PI(3,5)P2 on RyR2 channel activity, we measured the P_o of single RyR2 channels reconstituted in lipid bilayers. The RyR2 channels were activated by PI(3,5)P2 in a concentration-dependent manner, indicating that PI(3,5)P2 directly binds and regulates RyR2. These findings are consistent with those reported for skeletal muscle RyR1 channels (3). Our data indicate that PI(3,5)P2 acts on RyR2 by promoting the release of SR Ca^{2+} stores and by sensitizing the RyR2 to CICR.

Interestingly, although the mechanism of action of PI(3,5)P2 on RyR appears to be similar to skeletal muscle, the physiological consequence of this interaction seems to differ in cardiac muscle. We found $MIP^{-/-}$- and PI(3,5)P2-treated ventricular muscles to have enhanced contractility. In contrast, Shen *et al.* (3) reported significant reductions in peak isometric tension and a substantially "prolonged relaxation profile" following maximal contractions of the fast twitch extensor digitorum longus muscles from $MIP^{-/-}$. We believe our responses in cardiac muscle differ from skeletal muscle due to differences in the Ca^{2+}-handling properties between skeletal and cardiac muscle. In skeletal muscle, the ECC process operates via a mechanical coupling mechanism via the dihydropyridine receptor (DHPR) to trigger RyR1, without extracellular Ca^{2+} entry; therefore, PI(3,5)P2 likely depletes SR Ca^{2+} stores while the muscle is at rest. In contrast, we hypothesize that the influx of extracellular Ca^{2+} during cardiac muscle ECC helps maintain SR Ca^{2+} stores. Therefore, in cardiac muscle, PI(3,5)P2 may enhance RyR2 sensitivity to Ca^{2+} and promote greater SR Ca^{2+} release on a beat-to-beat basis by CICR. Nevertheless, studies specifically designed to directly compare skeletal and cardiac muscle function following PI(3,5)P2 manipulation are warranted.

Further, it remains to be determined whether elevation of PI(3,5)P2 is protective during cardiac disease or promotes the progression of cardiac pathologies. For example, our observed positive inotropic effects of PI(3,5)P2 could arguably help to preserve muscle force during a condition such as heart failure. Alternatively, increased Ca^{2+} leak from the SR may activate gene expression that contributes to heart failure. Moreover, it remains to be determined whether cardiac PI(3,5)P2 levels *in vivo* are altered by cardiac disease states or other stressors in the body. Importantly, there is evidence that PI(3,5)P2 levels can be acutely increased in the cell by exposure to environmental stressors such as hyperosmolarity (7) and UV light (8), endogenous agents such as interleukin-2 (8), and insulin (6). We were able to replicate these findings in HL-1 cardiomyo-

cytes, using insulin to increase the level of PI(3,5)P2. It is possible that PI(3,5)P2 levels may be altered by acute stressors such as exercise, inflammation, disease, or infection, which could regulate cardiac function.

In summary, our study provides evidence that PI(3,5)P2 is a potent regulator of $[Ca^{2+}]_i$ homeostasis by directly activating and sensitizing the RyR2 channel. We believe that this action of PI(3,5)P2 on the RyR2 causes additional release of Ca^{2+} during CICR, which can directly increase the strength of contraction in cardiac muscle.

REFERENCES

1. Di Paolo, G., and De Camilli, P. (2006) *Nature* **443,** 651–657
2. Shen, C., Lin, M. J., Yaradanakul, A., Lariccia, V., Hill, J. A., and Hilgemann, D. W. (2007) *J. Physiol.* **582,** 1011–1026
3. Shen, J., Yu, W. M., Brotto, M., Scherman, J. A., Guo, C., Stoddard, C., Nosek, T. M., Valdivia, H. H., and Qu, C. K. (2009) *Nat. Cell Biol.* **11,** 769–776
4. Hokin, L. E. (1985) *Annu. Rev. Biochem.* **54,** 205–235
5. McCrea, H. J., and De Camilli, P. (2009) *Physiology* **24,** 8–16
6. Berwick, D. C., Dell, G. C., Welsh, G. I., Heesom, K. J., Hers, I., Fletcher, L. M., Cooke, F. T., and Tavaré, J. M. (2004) *J. Cell Sci.* **117,** 5985–5993
7. Bonangelino, C. J., Nau, J. J., Duex, J. E., Brinkman, M., Wurmser, A. E., Gary, J. D., Emr, S. D., and Weisman, L. S. (2002) *J. Cell Biol.* **156,** 1015–1028
8. Jones, D. R., González-García, A., Díez, E., Martinez-A., C., Carrera, A. C., and Meŕida, I. (1999) *J. Biol. Chem.* **274,** 18407–18413
9. Bidlingmaier, S., and Liu, B. (2007) *Mol. Cell. Proteomics* **6,** 2012–2020
10. Yoon, H. Y., Miura, K., Cuthbert, E. J., Davis, K. K., Ahvazi, B., Casanova, J. E., and Randazzo, P. A. (2006) *J. Cell Sci.* **119,** 4650–4666
11. White, S. M., Constantin, P. E., and Claycomb, W. C. (2004) *Am. J. Physiol. Heart Circ. Physiol.* **286,** H823–H829
12. Hama, H., Torabinejad, J., Prestwich, G. D., and DeWald, D. B. (2004) *Methods Mol. Biol.* **284,** 243–258
13. Mulieri, L. A., Hasenfuss, G., Ittleman, F., Blanchard, E. M., and Alpert, N. R. (1989) *Circ. Res.* **65,** 1441–1449
14. Wacker, M. J., Kosloski, L. M., Gilbert, W. J., Touchberry, C. D., Moore, D. S., Kelly, J. K., Brotto, M., and Orr, J. A. (2009) *J. Pharmacol. Exp. Ther.* **331,** 917–924
15. Zhu, X., Ghanta, J., Walker, J. W., Allen, P. D., and Valdivia, H. H. (2004) *Cell Calcium* **35,** 165–177
16. Zhu, X., Zamudio, F. Z., Olbinski, B. A., Possani, L. D., and Valdivia, H. H. (2004) *J. Biol. Chem.* **279,** 26588–26596
17. Bertl, A., Blumwald, E., Coronado, R., Eisenberg, R., Findlay, G., Gradmann, D., Hille, B., Köhler, K., Kolb, H. A., and MacRobbie, E. (1992) *Science* **258,** 873–874
18. Suh, B. C., and Hille, B. (2008) *Annu. Rev. Biophys.* **37,** 175–195
19. Tanaka, H., Sekine, T., Nishimaru, K., and Shigenobu, K. (1998) *Comp. Biochem. Physiol. A Mol. Integr. Physiol.* **120,** 431–438